

Journal homepage: <http://civiljournal.semnan.ac.ir/>

## Numerical Investigation of Geometric Parameters Effect of the Labyrinth Weir on the Discharge Coefficient

**S. Emami<sup>1\*</sup>, H. Arvanaghi<sup>1</sup> and J. Parsa<sup>1</sup>**

1. Water Engineering Department, Faculty of Agriculture, University of Tabriz, Tabriz, Iran

Corresponding author: [somayhemami70@gmail.com](mailto:somayhemami70@gmail.com)

---

### ARTICLE INFO

Article history:

Received: 23 May 2017

Accepted: 09 July 2017

---

Keywords:

Labyrinth weir,

Discharge coefficient,

Computational fluid dynamics,

Fluent.

---

### ABSTRACT

Weirs, as overflow structures, are extensively used for the measurement of flow, its diversion and control in the open canals. Labyrinth weir due to more effective length than conventional weirs, allows passing more discharge in narrow canals. Determination the design criteria for the practical application of these weirs need more investigation. Weir angle and its position relative to the flow direction are the most effective parameters on the discharge coefficient. In this study, Fluent software was used as a virtual laboratory and extensive experiments were carried out to investigate the effect of geometry on the labyrinth weir discharge coefficient. The variables were the height of weir, the angle of the weir and the discharge. The discharge coefficients obtained from these experiments were then compared with the corresponding values obtained from the usual rectangular sharp crested weir experiments. Comparison of the results showed that in all cases with different vertex angle, flow discharge coefficients are in a satisfactory range for relative effective head less than 0.3. The discharge coefficient is decreased for relative effective head more than 0.3 due to the collision of water napes. It showed the higher weir, the more discharge capacity. As a result, the labyrinth weirs have a better performance in comparison with the common sharp crested.

---

## 1. Introduction

The labyrinth weir is one of the most economical weirs, because of its optimal discharge capacity in comparison with construction costs in other weirs. The great

advantages of linear crest weirs are their simplicity in construction and maintenance:

$$Q = \frac{2}{3} C_d \sqrt{2g} LH^{1.5} \quad (1)$$

where  $L$  = crest length of the weir,  $C_d$  = discharge coefficient,  $g$  = acceleration due to gravity and  $H$  = static head over the crest.

The  $C_d$  depends on the flow characteristics and geometry of the canal and weir (Kumar et al., 2013).

Several laboratory studies have been conducted on labyrinth weirs. Hay and Taylor (1970) examined various performances of labyrinth weirs. They studied the effect of bottom slope on overflow capacity of labyrinth weirs, and the influence of water head over the weir crest [2]. Darvas (1971) presented a definition for the discharge coefficient of labyrinth spillways. Houston and Hinchliff (1982) investigated the several labyrinth spillways for Hyrum dam by means of physical modeling of 45 different states. The study of Cassidy et al. (1985) on the performance of labyrinth spillways for high water head showed 20% reduction in efficiency of the spillways. Naseri (2003) compared discharge coefficient of labyrinth weirs for different crest shapes and lengths using physical modeling. He found that semi-circle crest shape has the highest discharge coefficient [3]. Carollo et al. (2012) also investigated the discharge capacity of triangular labyrinth weirs with different geometrical characteristics in a laboratory flume [3].

Emiroglu and Kisi (2013) predicted discharge coefficient of trapezoidal labyrinth side weirs using ANFIS. Results showed ANFIS model is more optimal.

Seamons (2014) worked on the effects of geometric design parameters of varying certain labyrinth weir to determine their effects on the discharge efficiency. The purpose of this study was to determine the effects of varying certain labyrinth weir geometric design parameters to determine the effects on discharge efficiency.

Roushangar et al. (2017) investigated the discharge coefficient of normal and inverted orientation labyrinth weirs using machine learning techniques. The results showed that  $Fr$  in the GEP model and  $Fr$  and  $H_T/P$  in the ANFIS model are the most effective variables for determining  $C_d$  for normal and inverted orientation labyrinth weirs, respectively.

Roushangar et al. (2017) applied support vector machine method to determine discharge coefficient of labyrinth and arced labyrinth weirs. Results of this study showed vector machine method is most effective method for obtaining discharge coefficient of labyrinth.

In recent years, progresses in computational fluid dynamics (CFD) algorithms and improvements in computer hardwares have resulted in evolving new tools for evaluation of different flow conditions and different design alternatives. Savage et al. (2004) and Danish hydraulic institute (DHI) (2005) studied the flow past the labyrinth spillways using numerical simulation. Crookston (2012) performed numerical simulation on the multi-dimensional labyrinth weirs. They used a previous physical model results on a rectangular flume under laboratory conditions. They performed, then, a three-dimensional simulation of flow over the weir using Flow-3D Software. The objective of their study was showing the capability of Reynolds Averaged Navier-Stokes equations in the modeling of flow turbulence over the Labyrinth weirs. Due to the importance of accurate modeling of the free-surface, a two-phase flow, i.e. water and air, was utilized. Thus, the robust volume of fluid (VOF) technique was used to determine the location and orientation of the interface between the water and air, i.e. free surface.

In this paper, we examined the effects of the geometric parameters on the discharge coefficient of labyrinth weirs. This study is aimed to specify a range for the geometric parameters in which the weir discharge coefficient remains constant.

## 2. Materials and methods

### 1.2. Labyrinth Weir

Labyrinth weirs are very easy to design and have more effective length than the common sharp crested weirs. They would be able to pass more discharge in comparison with the usual weirs for the same length and head of water. Figure (1) shows a sketch of Labyrinth weir,

related parameters, and the section view of flow over the weir.

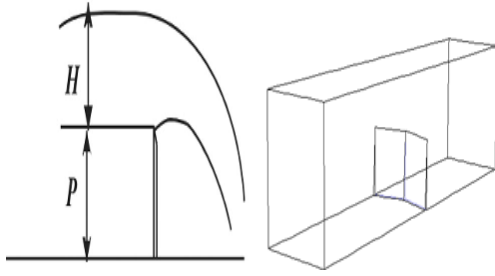


**Figure 1.** Labyrinth weir and the corresponding parameters; (a) plan view; (b) section view of flow over Labyrinth weir.

## 2.2. Governing Equations

The governing equations of flow over weirs are the well-known Navier- Stokes equations; a continuity equation and three momentum equations in the three-dimensional state. By including the effect of turbulence, the equations change to Reynolds equations as [Wilcox and David, 2006]:

Continuity equation:

$$\frac{\partial u_i}{\partial x_i} = 0 \quad (2)$$

Momentum equation:

$$\rho \frac{\partial u_i}{\partial x_i} + \rho \frac{\partial}{\partial x_j} (U_j U_i + \overline{u'_j u'_i}) \quad (3)$$

in which  $U_i$  is average velocity in (i) direction,  $P$  is pressure,  $\mu$  is Molecular viscosity,  $\rho$  is density of water,  $S_{ji}$  is Strain-rate tensor,  $\overline{u'_j u'_i}$  istime-averaged momentum due to turbulence which is called Reynolds stresses.  $\overline{\rho u'_i u'_j}$  has nine components [Wilcox and David,2006]:

$$\overline{\rho u'_i u'_j} = \begin{bmatrix} \overline{\rho (u'_1)^2} & \overline{\rho u'_1 u'_2} & \overline{\rho u'_1 u'_3} \\ \overline{\rho u'_2 u'_1} & \overline{\rho (u'_2)^2} & \overline{\rho u'_2 u'_3} \\ \overline{\rho u'_3 u'_1} & \overline{\rho u'_2 u'_3} & \overline{\rho (u'_3)^2} \end{bmatrix} \quad (4)$$

These unknowns, due to the turbulence, are determined by using turbulence models. These models consist of semi-empirical equations which relate the fluctuating components of quantities to the average components. The most popular turbulence model is k- $\epsilon$  model. The

RNG scheme of this model can be used to solve Reynolds stresses.

There are different methods to solve RANS equations. In this study, k- $\epsilon$  RNG turbulence model is used which is defined as (Papageorgakis and Assanis, 1999):

$$\frac{\partial}{\partial t} (\rho k) + \frac{\partial}{\partial x_i} (\rho k u_i) = \frac{\partial}{\partial x_j} \left( \alpha_k \mu_{\text{eff}} \frac{\partial k}{\partial x_j} \right) + G_k + G_b - \rho \epsilon - Y_M + S_k \quad (5)$$

$$\frac{\partial}{\partial t} (\rho \epsilon) + \frac{\partial}{\partial x_i} (\rho \epsilon u_i) = \frac{\partial}{\partial x_j} \left( \alpha_\epsilon \mu_{\text{eff}} \frac{\partial \epsilon}{\partial x_j} \right) + C_{1\epsilon} \frac{\epsilon}{k} (G_k + C_{3\epsilon} G_b) - C_{2\epsilon} \rho \frac{\epsilon^2}{k} - R_\epsilon + S_\epsilon \quad (6)$$

where  $k$  is kinetic energy,  $\epsilon$  is energy dissipation rate,  $G_k$  is turbulence kinetic energy generation due to mean velocity gradient,  $G_b$  is kinetic energy due to floatation,  $Y_M$  is turbulence Mach number and the other parameters are model coefficients and:

$$R_\epsilon = \frac{C_\mu \rho \eta^3 \left(1 - \frac{\eta}{\eta_0}\right) \epsilon^2}{1 + \beta \eta^3 k} \quad (7)$$

$$C_\eta = \frac{\eta \left(1 - \frac{\eta}{\eta_0}\right)}{1 + \beta \eta^3} \quad (8)$$

These unknowns are determined by using turbulence modeling process. (3)

## 3.2. Volume of Fluid (VOF) Approach

This approach was first introduced by Hirt and Nichols in 1981 (Hirt et.al, 1981). In this approach, the fraction of computational cells occupied by each fluid, e.g. water and air, and the position of the interface between fluids were determined. The location of the interface is calculated using the following equations (Chen et. al, 2002):

$$\frac{\partial \alpha_w}{\partial t} + u_i \frac{\partial \alpha_w}{\partial x_i} = 0 \quad (9)$$

$$\alpha_a = 1 - \alpha_w \quad (10)$$

Which  $\alpha_w$  and  $\alpha_a$  are respectively the fractions of water and air within a cell. The above equations are for a two-phase flow which consists of water and air; the subscript "w" refers to water and "a" refers to air. The

momentum equation for this two-phase flow is similar to that of for a single flow which expressed by Navier- Stokes equations. But  $\rho$  (density) and  $\mu$  (molecular viscosity) should be modified due to the variations of each fluid fraction. Thus, they may be written as (Anonymous, 2006):

$$\rho = \alpha_w \rho_w + (1 - \alpha_w) \rho_a \quad (11)$$

$$\mu = \frac{\alpha_w}{\mu_w} + (1 - \alpha_w) \mu_a \quad (12)$$

in which,  $\rho_a$  and  $\rho_w$  are density of air and water, while  $\mu_a$  and  $\mu_w$  are the molecular viscosity of air and water, respectively (Anonymous, 2006).

#### 4.2. Numerical Solution

In this study, numerical modeling is carried out by Fluent v. 6.2. Fluent is one of the powerful and common CFD commercial software. It first transforms the governing equations to the algebraic equations by finite volume method then solves them. Fluent has the ability to solve 2D and 3D problems of open canal flow, confined conduit flow and sediment transport by the turbulence models. Also, it is possible to solve continuum and momentum equations so called Navier- Stocks equations around Labyrinth weirs. The experiments were conducted in a canal of length 4.5 m, width 0.5 m and depth 0.6 m. To solve the partial differential governing equations, fluent employs the Finite Volume Method. Discretization of the governing equations can be done by applying the upwind method. The simulated velocity and pressure fields are coupled by using "Piso" method. To start Fluent modeling, we first need to specify canal geometry and then generate a mesh for it. Gambit software is used to generate the mesh. GAMBIT Software is used for geometrical construction and grid generation of numerical model through which user can depict and generate grids for considered model with the highest accuracy. This software has a set of commands for rapid organization of 2D and 3D geometries. It also includes structural and

unstructured meshes. In general, the generation of grids in GAMBIT is carried out as:

1. Creating the geometry of problem
2. Generating the grid of created geometry
3. Defining the related boundary conditions
4. Meshing the geometrical model of labyrinth weir using Gambit is shown in Figure (2).

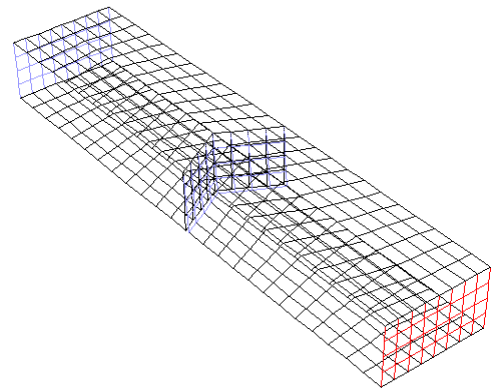


**Figure2.** Meshing the geometrical model of Labyrinth weir using GAMBIT

Suitable boundary conditions are of primary importance. These are shown in Figure (3).

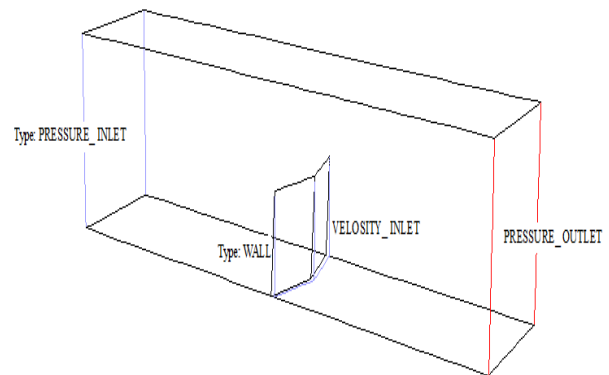


**Figure3.** Boundary conditions used in simulation throughout the domain

A water inlet: pressure inlet boundary condition was used to define the water pressure at flow inlets. This boundary condition is based on the assumption that upstream inlet is

sufficiently far away from the crest where velocity is negligible. For the leading walls at two sides of flow as well as for the bottom, the wall boundary condition is assigned to bound fluid and solid regions. For downstream, a pressure outlet boundary was considered to specify static pressure at outlet.

Discharge equation for a labyrinth weir can be obtained a:

$$Q = \frac{2}{3} C_d L \sqrt{2g} H_0^{3/2} \quad (13)$$

In which,  $L$  and  $H_0$  are the effective length of weir and total head on the crest, respectively.  $L$  is defined according to the geometry of the weir and total head ( $H_0$ ) is defined as the summation of static head ( $P/\rho g$ ) and velocity head ( $U^2/2g$ ) that are determined once the pressure and velocity fields are computed by numerical solution. Then, the discharge coefficient,  $C_d$ , can be obtained (Zahraeifard V and Talebeydokhti, 2012).

## 5.2. Dimensional analysis

The flow discharge of the weir is a function of several parameters (Figure 1), which is

mathematically expressed by the following equation:

$$C_d = f(H_d, L_e, P, W, \theta, y) \quad (14)$$

Where  $H_d$  is the total head over the weir crest,  $W$  is the weir width,  $P$  is the height of the weir,  $\theta$  is the vertex angle and  $y$  is the flow depth. A dimensional analysis is performed to find a relation between the discharge coefficient and other parameters stated above. Below a mathematical expression of this relation is given:

$$C_d = f\left(F_r, \frac{H_d}{P}, \frac{L_e}{P}, \frac{y}{P}, \frac{H_d}{w}, \frac{y}{w}, R_e, \frac{L_e}{w}, \theta, W_e\right) \quad (15)$$

## 3. Results and discussions

The numerical simulations were performed for the weirs of vertex angle  $\theta = 30^\circ, 60^\circ, 90^\circ, 120^\circ, 150^\circ$  and  $180^\circ$  and two different heights of Labyrinth weirs of the same width of the canal. The ranges of the data are given in Table 1.

**Table1.** Results of the simulations in the present study

No.	$\Theta$ (°)	L (m)	H (m)	P (m)	H/P	$C_d$	Q (L/S)
W1	45	1.32	0.03	0.3	0.1	0.992	20.1926
W2	45	1.32	0.05	0.3	0.17	0.720	31.5345
W3	45	1.32	0.1	0.3	0.33	0.509	63.0545
W4	45	1.32	0.15	0.3	0.5	0.530	103.094
W5	45	1.32	0.2	0.3	0.67	0.730	154.1686
W6	60	1	0.03	0.3	0.1	1.030	15.8834
W7	60	1	0.05	0.3	0.17	0.809	26.8428
W8	60	1	0.1	0.3	0.33	0.517	48.5193
W9	60	1	0.15	0.3	0.5	0.473	81.5497
W10	60	1	0.2	0.3	0.67	0.460	120.776
W11	90	0.7	0.03	0.3	0.1	1.130	12.1978
W12	90	0.7	0.05	0.3	0.17	1.007	23.3887
W13	90	0.7	0.1	0.3	0.33	0.690	45.3285
W14	90	0.7	0.15	0.3	0.5	0.570	68.7914
W15	90	0.7	0.2	0.3	0.67	0.550	102.1951
W16	120	0.57	0.03	0.3	0.1	1.230	10.8115
W17	120	0.57	0.05	0.3	0.17	1.060	20.0475

W18	120	0.57	0.1	0.3	0.33	0.775	41.4573
W19	120	0.57	0.15	0.3	0.5	0.662	65.0570
W20	120	0.57	0.2	0.3	0.67	0.625	94.4636
W21	150	0.52	0.03	0.3	0.1	1.280	10.2641
W22	150	0.52	0.05	0.3	0.17	1.120	19.3242
W23	150	0.52	0.1	0.3	0.33	0.800	39.041
W24	150	0.52	0.15	0.3	0.5	0.721	64.6398
W25	150	0.52	0.2	0.3	0.67	0.671	92.6180
W26	180	0.5	0.03	0.3	0.1	1.132	10.1778
W27	180	0.5	0.05	0.3	0.17	1.153	19.1284
W28	180	0.5	0.1	0.3	0.33	0.812	38.1022
W29	180	0.5	0.15	0.3	0.5	0.730	62.9295
W30	180	0.5	0.2	0.3	0.67	0.684	90.7811

Variation of  $C_d$  with  $H/P$  is shown in Fig. 4 for the weirs of different vertex angles. It can be noted that  $C_d$  decreases by decreasing the vertex angle due to collision of the falling jets for high value of  $H/P$ . However, for the low value of  $H/P$ , the collision of jets is not so severe, resulting in high values for  $C_d$ . As a result, by increasing the vertex angle, the decrease rate of  $C_d$  with  $H/P$  decreases.

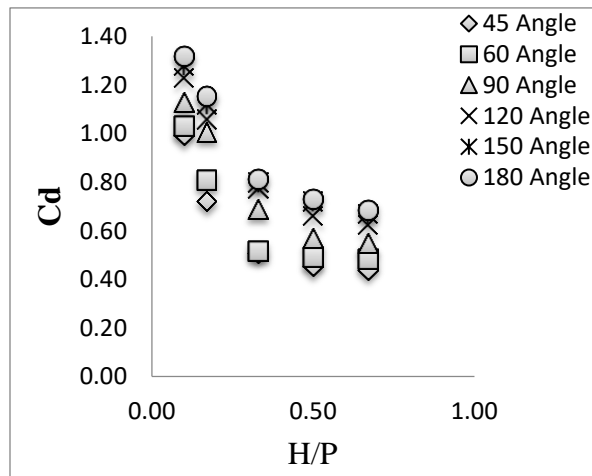


**Figure4.** The Numerical results of the  $C_d$  at various  $\theta$

Variation of discharge with head over the crest for the Labyrinth weirs of different vertex angles is shown in Fig. 5. This figure indicates that for the same value of  $h$ , discharge

increases with the decrease of vertex angle due to increase of the crest length of the weir.

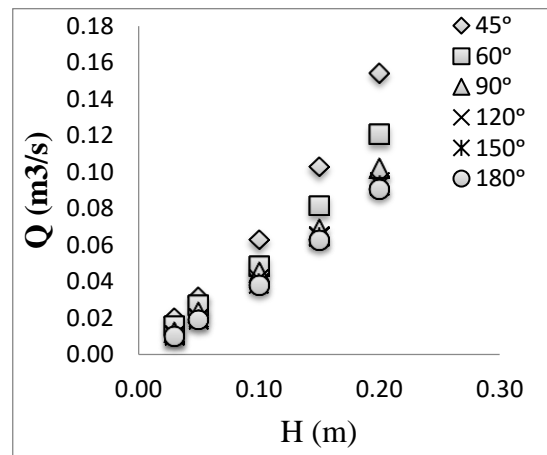


**Figure5.** Variation of  $Q$  with  $H$  for Labyrinth weir of different vertex angle

### 3.1. The effect of the height of weir on discharge coefficient

Figure 5 and 6, represents the dimensionless height of weir effect on the discharge coefficient. As seen from figure 6 and 7, by increasing the height of weir, the discharge coefficient increase and the value of discharge coefficient is constant after  $H/P = 0.3$  and is fixed by 0.47.

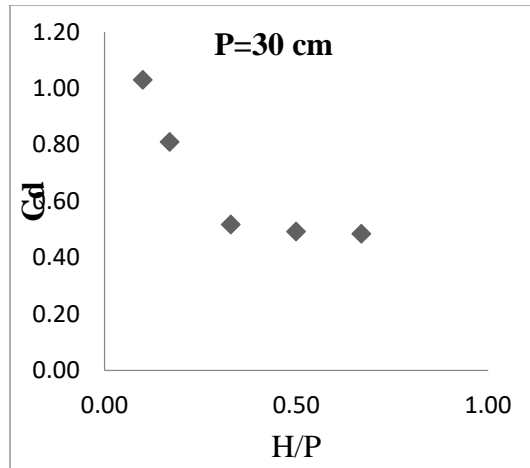


**Figure6.** The Numerical results of the  $C_d$  at various H/P (P=30 cm)

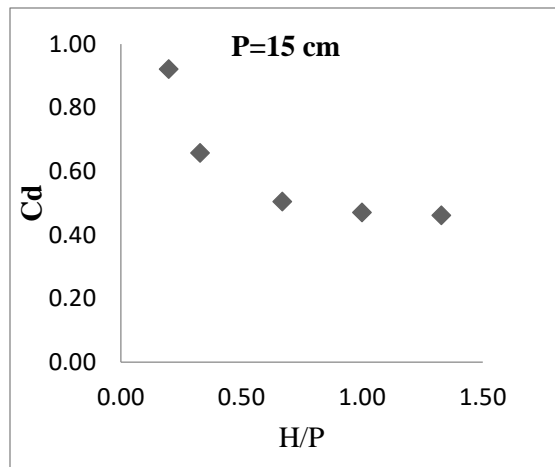


**Figure7.** The Numerical results of the  $C_d$  at various H/P (P=15 cm)

### 3.2. Efficiency of the Labyrinth weir

A more hydraulic criteria for selecting a proper weir, is its flow capacity in the same conditions, e.g. water head and weir length. To examine the efficiency of Labyrinth weir for different vertex angles, ratio of discharges over the Labyrinth weir to the discharges over usual rectangular sharp crested weir, i.e. increase flow percent (Q%), is represented with H/P in Fig. 8. The efficiency of Labyrinth weir is high

for low vertex angle. It decreases with increase of H/P due to collision of the falling jets. For H/P= 0.3, the efficiency of Labyrinth weir is low and even for  $\theta = 45^\circ$ , the efficiency is only 1.5 times to the usual rectangular sharp crested weir.

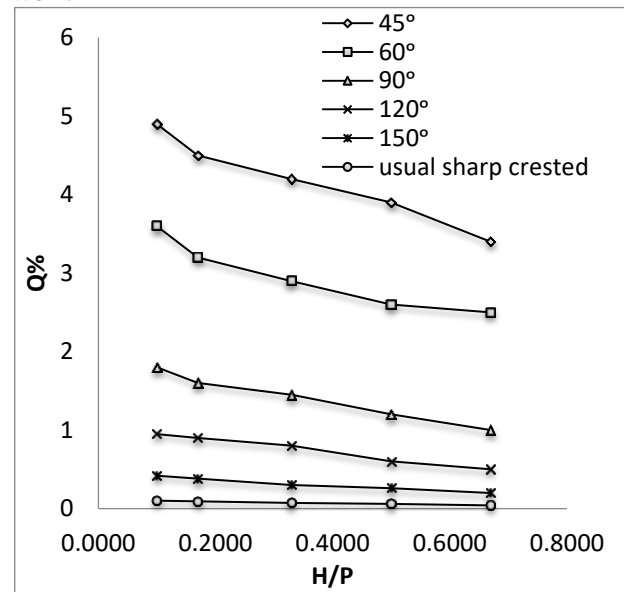


**Figure8.** Comparison variation of Q% with H/P for the Labyrinth weir of different vertex angle and usual sharp-crested weir

### 3.3. Discharge equation for Labyrinth weir

Based on the obtained fitting of the resulted data by the numerical model, discharge coefficient equation for Labyrinth weir can be obtained as follows:

$$C_d = 0.0948 \left(\frac{H}{P}\right)^{-0.249} \theta^{0.374} \quad (16)$$

As observed in the equation, determination coefficient of the equation equals 96% (which is acceptable) using linear fitness.

Above equation, with error value of 0.01695; was presented as the best equation to estimate the discharge coefficient over duckbill weirs. The application range of this equation is  $45^\circ \leq \theta \leq 180^\circ$  and  $0.1 \leq \frac{H}{P} \leq 0.67$ .

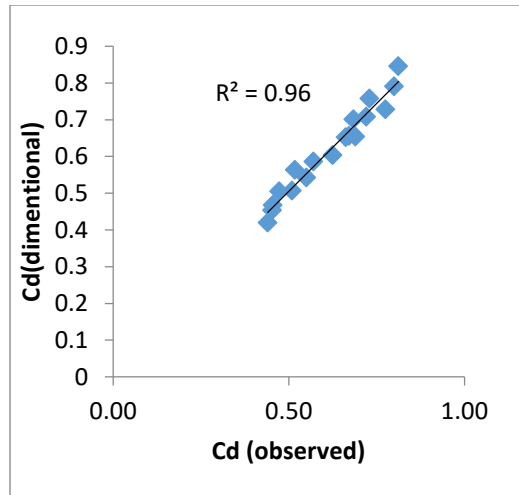


**Figure9.** The predicted values of the  $C_d$  at various observed values of  $C_d$

#### 4. Conclusions

Labyrinth weir is a kind of non-linear weirs which are used to control and measure the flow in open channels where the width of channel is low. In this study we investigated the effects of Labyrinth weir geometric parameters on the discharge coefficient. To do this, Fluent software was used, as a virtual laboratory, in order to simulate the different conditions of alabyrinth weir. The variables were the height of weir, the angle of the weir and the discharge. The results indicated that the discharge coefficient decreases with the vertex angle. However, for low values of  $H/p$  and vertex angle, the  $C_d$  is high. By increasing the height of weir, the discharge coefficient increase and the value of discharge coefficient remains 0.47 for  $H/P > 0.3$ . The regression analysis showed that the vertex angle of the weir is the most important design parameter for labyrinth weirs. The efficiency of the Labyrinth weir is high for low vertex angle and it decreases with increase of  $H/P$  due to the collision of the falling jets.

#### References

- [1] Hirt, C. W. and Nichols, B. D. (1981). "Volume of Fluid (VOF) Method for the Dynamics of Free 274 Boundaries", *Journal of Comput. Phys*, Vol. 39(1), pp. 201-225.
- [2] Kumar, S., Ahmad, Z., Mansoor, T and Himanshu, S. K. (2013). "A New Approach to analyze the flow over sharp crested curved plan form weir." *International Journal of Recent Technology and Enginnering (IJRTE)*, Vol. 2, pp. 2277-3878.
- [3] Hay, N., Taylor, G. (1970). "Performance and design of labyrinth weirs." *ASCE, Journal of Hydraulics Division*, Vol. 96(11), pp. 2337-57.
- [4] Crookston B. M., Paxson, G. S. and Savage, B. M. (2012). "Hydraulic performance of labyrinth weirs for high headwater ratios. 4th IAHR". *International Symposium on Hydraulic Structures*, Porto, Portugal, pp. 1-8.
- [5] Shaghaghian R. S., Sharif, M. T. (2015). "Numerical modeling of sharp-crested triangular plan form weirs using FLUENT." *Indian Journal of Science and Technology*, Vol. 8(34), DOI: 10.17485/ijst/2015/v8i34/78200.
- [6] Emiroglu, M. E., Kisi, O. (2013). "Prediction of discharge coefficient for trapezoidal labyrinth side weir using a neuro-fuzzy approach." *Water Resources Management*, Vol. 27(5), pp. 1473-1488.
- [7] Seamons, T. R. (2014). "LabyrinthWeir: A look into geometric variation and its effect on efficiency and design method predictions." M. S. thesis, Utah State University, Logan, UT.



- [8] Roushangar, K., Alami, M. T., MajediAsl, M. and Shiri, J. (2017). "Modeling discharge coefficient of normal and inverted orientation labyrinth weirs using machine learning techniques." *ISH Journal of hydraulic engineering*.  
Homepages://www.tandfonline.com/loi/tish20.
- [9] Roushangar, K., Alami, M.T., Shiri, J. and MajediAsl, M. (2017). "Determining discharge coefficient of labyrinth and arced labyrinth weirs using support vector machine." *Journal of Hydrology Research*, Available Online: 2017 Mar, nh2017214; DOI: 10.2166/nh.2017.214.
- [10] Papageorgakis G. C., Assanis, D. N. (1999). "Comparison of linear and nonlinear RNG-based models for incompressible turbulent flows." *Journal of Numerical Heat Transfer*, University of Michigan, Vol. 35, pp. 1-22.
- [11] Wilcox., David, C. (2006). "Turbulence Modeling for CFD." DCW Industries, Inc., La Canada, CA, 270 USA.
- [12] Zahraeifard, V. and Talebeydokhti, N. (2012). "Numerical Simulation of Turbulent Flow over Labyrinth Spillways/Weirs." *International Journal of Science and Tecnology*, Vol. 22(5), pp.1734-1741.
- [13] Anonymus. (2006). "Fluent 6.3 User's Guide. Chap. 23. Fluent Incorporated." Lebanon.
- [14] Danish Hydraulic Institute website (DHI)<<http://ballastwater.dhigroup.com/> 268 /media/publications/news/2009/07059ns3.pdf>. (Visited Aug. 17, 2010).
- [15] Savage, B. M., Frizell, K. and Crowder, J. (2004). "Brains versus Brawn: The Changing World of 265 Hydraulic Model Studies". *Proc. of the ASDSO Annual Conference*, Phoenix, AZ, USA 266.